# Prethermalization via self driving and external driving of extensive subsystems

Finn Lasse Buessen , 1,\* Hyun-Yong Lee, 2,3,4,\* Tarun Grover, 5 and Yong Baek Kim<sup>1,†</sup>

<sup>1</sup>Department of Physics, University of Toronto, Toronto, Ontario M5S 1A7, Canada

<sup>2</sup>Department of Applied Physics, Graduate School, Korea University, Sejong 30019, Korea

<sup>3</sup>Division of Display and Semiconductor Physics, Korea University, Sejong 30019, Korea

<sup>4</sup>Interdisciplinary Program in E·ICT-Culture-Sports Convergence, Korea University, Sejong 30019, Korea

<sup>5</sup>Department of Physics, University of California at San Diego, La Jolla, California 92093, USA

(Received 25 February 2022; revised 29 September 2022; accepted 7 November 2022; published 16 November 2022)

We investigate the nonequilibrium states of an interacting multicomponent quantum system when only an extensive subsystem is quantum quenched or driven from the ground state. As a concrete example, we consider a system where two XXZ spin chains are coupled to a transverse field Ising (TFI) chain, and only the transverse field in the TFI chain is quantum quenched or periodically driven in time, starting from an initially ordered state. This system is studied using density matrix renormalization group simulations and various entanglement entropy diagnostics. In the case of quantum quenching, when the transverse field is suddenly switched on to become the largest energy scale, the resulting internal dynamics leads to a prethermal steady state with persistent oscillating magnetization ("self driving") and emergent conservation laws. Upon applying the time-dependent drive to the TFI chain ("external driving"), sufficiently fast drive gives rise to a prethermal steady state with finite magnetization, whereas a slow drive generates a high-temperature disordered state. We briefly discuss the experimental implementation of our protocol in organic materials with quantum-tunneling hydrogen atoms.

quantum systems.

DOI: 10.1103/PhysRevB.106.174417

### I. INTRODUCTION

Our ability to understand nonequilibrium quantum states of interacting quantum matter would significantly expand the scope of accessible quantum phases of condensed matter and cold atom systems [1-3]. Of particular interest are the prethermal states that may persist for an exponentially long period of time and arise as a consequence of emergent quasiconservation laws. For example, in closed systems, the Floquet-type (periodic in time) drive may, in general, heat up the system to the infinite-temperature state [4–6]; however, the integrable systems [7,8] and many-body localized (MBL) systems [9-11] show prethermal steady states in accordance with associated conserved quantities. Alternatively, quantum quenching in certain systems may lead to quasiconserved quantities, which can then give rise to long-lived prethermal steady states. Yet, most of the previous studies are limited to cases in which the entire system is quenched or driven together (see, e.g., Refs. [2,12–15]). Many condensed matter and cold atomic systems, however, consist of multiple degrees of freedom, and different parts of the system may possess distinct natural time scales. In this setting, one may ask whether quenching or driving only a subsystem would necessarily heat up the entire system or whether there may be a different limit in which nontrivial dynamic states can be realized. Moreover, we may also ask how one could effectively characterize the

becomes the largest intrinsic energy scale, the entire system

enters a prethermal state with oscillating magnetization in

both the XXZ and TFI chains. We explain this phenomenon by constructing an effective Hamiltonian where emergent decoupling between the XXZ and TFI chains occurs and new quasiconservation laws arise. Next, by imposing a periodic drive on the transverse field in the TFI chain and starting from

an ordered ground state of the whole system, we investigate

nonequilibrium states in such subsystem-driven interacting

two XXZ spin chains are coupled to a transverse field Ising

(TFI) spin chain and only the latter is quenched or driven by a

time-dependent transverse field; see the schematic illustration

in Fig. 1. This model is partially motivated by the theory

of organic materials in which layers of electronic degrees of

freedom are coupled via hydrogen bonds; quantum tunneling

between the bistable ground-state configurations of the hy-

drogen bonds can then be modeled by transverse field Ising

spins [16,17]. Using the density matrix renormalization group

In this paper, we consider an interacting spin model, where

<sup>(</sup>DMRG), we study both equilibrium and nonequilibrium scenarios in our model. First, we establish the equilibrium phase diagram as a function of the time-independent transverse field strength in the TFI chain and the exchange interaction scales in the system. It is demonstrated that there exists a direct transition from an ordered state (ordered in both the XXZ and TFI subsystems) to a fully quantum disordered state, where neither of the subsystems shows finite magnetization. We then consider a quantum-quench protocol where a large transverse field in the TFI chain is suddenly turned on, starting from an ordered ground state. It is found that when the transverse field

<sup>\*</sup>These authors contributed equally to this work.

<sup>†</sup>ybkim@physics.utoronto.ca

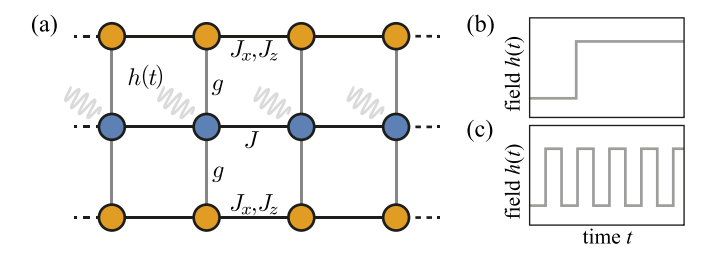


FIG. 1. Coupled three-chain model. (a) The top and bottom chains (yellow sites) are XXZ models with exchange constants  $J_x$  and  $J_z$ . The middle chain (blue sites) is a TFI chain with interaction J and on-site time-dependent transverse field h(t). The chains interact via a term  $g\sigma_i^z(\sigma_{i,t}^z - \sigma_{i,b}^z)$ ; see text for details. (b) Quench protocol with a sudden onset of the transverse field. (c) Periodic driving protocol.

how the resulting nonequilibrium state evolves as a function of the driving frequency. We demonstrate that the low- and high-frequency drives of the TFI subsystem lead to very different behaviors of the composite model. We show that if the drive frequency is sufficiently large, the system may remain in a long-lived, symmetry-broken prethermal regime and maintain its finite magnetization. Remarkably, the polarizable environment of XXZ chains significantly enhances the stability of the prethermal regime when compared with an isolated TFI chain.

#### II. MODEL

We investigate a model of three coupled spin chains that consists of a transverse field Ising (TFI) chain at the center and two XXZ spin chains at the top (t) and bottom (b) of the system as illustrated in Fig. 1. The Hamiltonian of the full system reads  $H = H_{\text{TFI}} + H_{\text{XXZ},t} + H_{\text{XXZ},b} + H_{\text{int}}$ , where the TFI and XXZ terms are given by

$$H_{\text{TFI}} = J \sum_{\langle i,j \rangle} \sigma_i^z \sigma_j^z + h(t) \sum_i \sigma_i^x,$$

$$H_{\text{XXZ},\alpha} = \sum_{\langle i,j \rangle} J_x \left( \sigma_{i,\alpha}^x \sigma_{j,\alpha}^x + \sigma_{i,\alpha}^y \sigma_{j,\alpha}^y \right) + J_z \sigma_{i,\alpha}^z \sigma_{j,\alpha}^z. \quad (1)$$

Here,  $\langle i, j \rangle$  denote nearest-neighbor lattice sites i and j within each chain,  $\alpha = t$ , b discriminates the top and bottom chain, and  $\sigma^{\gamma}$  are the Pauli matrices with  $\gamma = x, y, z$ . The three spin chains are locally coupled via an interaction term  $H_{int}$  =  $g\sum_{i}\sigma_{i}^{z}(\sigma_{i,t}^{z}-\sigma_{i,b}^{z})$ , which couples the local magnetization  $\sigma_{i}^{z}$ of the TFI chain to the local magnetization difference of the two XXZ chains via the interaction constant g. In addition to the symmetries corresponding to the U(1) rotation about the z axis separately in the top and bottom chains, there exists also a global Ising symmetry corresponding to  $\sigma_i^z \mapsto$  $-\sigma_i^z, \sigma_{i,\alpha}^z \mapsto -\sigma_{i,\alpha}^z$ . Note that the top and bottom XXZ chains do not interact directly. We fix J = 1,  $J_x = 1$ , and g = 0.5and investigate the role of varying h(t) and  $J_z$  in this paper. Our rationale behind fixing J = 1 and  $J_x = 1$  is to induce two inherently different types of spin chains that nonetheless have the same characteristic energy scale: Both the TFI chain and the XXZ chains exhibit quantum phase transitions at h = 1and  $J_z$ , respectively, between their ordered and disordered phases. Similarly, choosing an interchain coupling of g = 0.5ensures that the dominant energy scale is set by the interaction

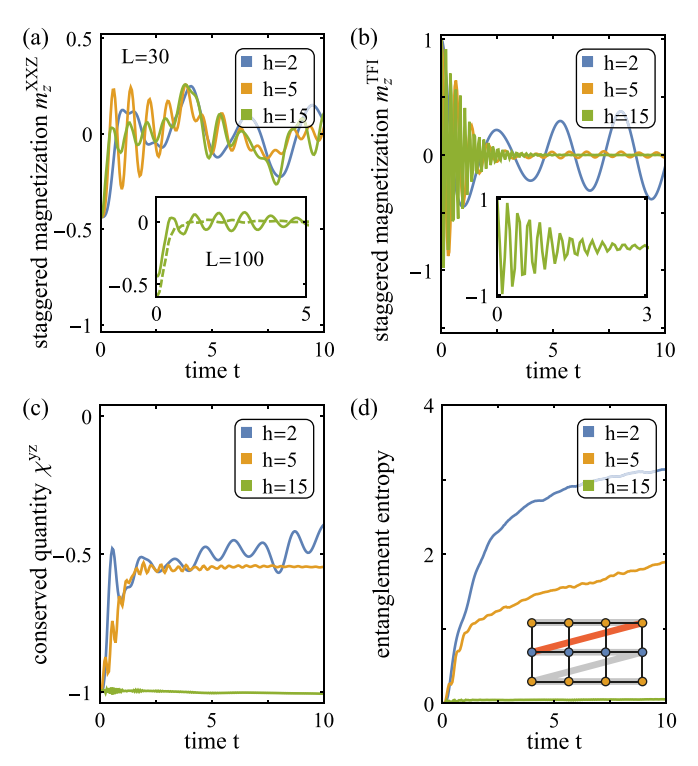


FIG. 2. Quench dynamics after a sudden shift in the magnetic field from h=0 to various values h=2,5,15. Data shown are for finite chain length L=30 with periodic boundary conditions, interaction  $J_z=0$ , and maximum bond dimension  $\chi_{\rm max}=512$ . (a) Evolution of the staggered magnetization in the XXZ subsystem. The inset shows data for larger system size L=100. The dashed line depicts data for  $J_z=0.5$ . (b) Staggered magnetization in the TFI chain. The inset shows the short-time dynamics for h=15. (c) Conserved quantity  $\chi^{\rm yz}$  in the TFI chain. (d) Bipartite entanglement entropy at the cut between the (top) XXZ chain and the remainder of the system; these data are for L=10 and  $\chi_{\rm max}=1024$ . The inset illustrates the layout of the MPS using thick gray lines; the bipartitioning cut is colored red.

within each individual chain; yet it remains non-negligible in determining the qualitative behavior of the system. Such intermediate coupling strength is believed to be appropriate for the modeling of hydrogen-bond-mediated exchange between electronic degrees of freedom in organic materials [17]—a class of materials that inspired our model Hamiltonian in Eq. (1).

## III. METHOD

Our calculations of the equilibrium ground state are based on the density matrix renormalization group (DMRG) method [18–20]. For this purpose, unless indicated otherwise, the three-chain model is mapped onto a one-dimensional matrix product state (MPS) by winding the MPS along the first XXZ chain, then along the TFI chain, and finally along the second XXZ chain [see inset of Fig. 2(d)]. To study the quantum quench or periodic driving from the ground states, we employ the time-dependent variational principle (TDVP) [21]. For characterizing the entanglement between different subsystems, in addition to more conventional

measures, we calculate the "quantum disentanglement liquid" (QDL) diagnostic [22–25]. The QDL diagnostic is designed to extract an effective entanglement between two subsystems of a tripartite system: We consider the whole system as a union of three subsystems A, B, and C and project the subsystem C into a given basis state,  $X \equiv \{x_c\}$ , resulting in a state  $|\psi_{AB}^X\rangle \equiv \bigotimes_{c \in C} \langle x_c | \psi \rangle$ . Then, the QDL diagnostic is defined as  $S_{\text{QDL}} \equiv \sum_X p_X S_{AB}^X$ , where  $p_X \equiv \langle \psi_{AB}^X | \psi_{AB}^X \rangle$  and  $S_{AB}^X \equiv -\text{Tr}(\rho_A^X \ln \rho_A^X)$  is the entanglement entropy (EE) of the reduced density matrix  $\rho_A^X \equiv \text{Tr}_B(|\psi_{AB}^X\rangle\langle\psi_{AB}^X|)$ . Consequently, the QDL diagnostic reflects an effective entanglement between subsystems A and B, and as shown in Ref. [25] it also bounds the conditional entanglement between the subsystems. See Supplemental Material (SM) for further details on the QDL diagnostic [26].

#### IV. GROUND-STATE PHASE DIAGRAM

We first carve out the ground-state phase diagram of the three-chain model as a function of  $h \equiv h(t)$  and  $J_z$ . We observe two possible ground-state phases of the three-chain model. At small values for the transverse field  $h \ (< J)$ , or large values of  $J_{z}$  (>  $J_{x}$ ), the ground state is a composite magnetic order where the global Ising symmetry is broken and all three chains obtain a finite magnetization along the z axis. In the opposite limit, i.e., h > J and  $J_z < J_x$ , the magnetization vanishes across all three chains as they remain disordered; note that in this parameter regime the chains would also be disordered in the absence of any interchain interaction, i.e., g = 0, where the XXZ (TFI) chains form a Luttinger liquid (paramagnet) [27–30]. The detailed phase diagram is discussed in the SM. We note that our ground-state phase diagram has strong resemblance to that for models of organic materials such as  $\kappa$ -H<sub>3</sub>(Cat-EDT-TTF)<sub>2</sub> [16,17], whereby the XXZ chains play the role of electronic spins, while the TFI chain spins play the role of hydrogen atoms tunneling in a double-well potential.

## V. "SELF-DRIVEN" PRETHERMALIZATION VIA QUANTUM QUENCHING

We imagine a scenario where we start from an ordered ground state of the entire system at vanishing transverse field in the TFI chain and then suddenly change the transverse field to become finite—a so-called quantum quench [schematically depicted in Fig. 1(c)]. In this setting we shall investigate the time evolution of the magnetization in the XXZ chains for various strengths of the transverse field. While for small transverse field strength the time evolution is expected to be chaotic and therefore difficult to predict in detail, we are able to formulate an analytically reasoned expectation for the case when the transverse field is much larger than all other interaction scales in the system. For our analysis we employ the following mapping [31,32]. Let us write  $H = h \sum_{i} \sigma_{i}^{x} + V$  and utilize the interaction picture with V treated as a perturbation to the transverse field term. The interaction picture many-body wave function  $|\psi^I(t)\rangle$  is given by  $i\frac{d|\psi^I(t)|}{dt} = V^I(t)|\psi^I(t)\rangle$ , where  $V^I(t) = U(t)VU(t)^\dagger$  and  $U(t) = \exp(ith\sum_i \sigma_i^x)$ . As one may readily check, U(t+1) $2\pi/h$ ) = U(t), and thus  $V^{I}(t)$  is time periodic with frequency  $\omega \equiv T^{-1} = h/2\pi$ , despite H not having any such periodicity. One can now borrow the results on prethermalization in time-periodic systems [31–34] to understand the behavior of  $|\psi^I(t)\rangle$ . The essential point is that when h is much larger than all other intrinsic energy scales in the problem, then for times that are exponential in h, the interaction picture wave function  $|\psi^I(t)\rangle$  will evolve with an effective, time-independent Hamiltonian  $V_{\rm eff} = \overline{V^I(t)}$  that equals the time-averaged  $V^I(t)$ . Explicitly,  $|\psi^I(t)\rangle = e^{-iV_{\rm eff}\,t}|\psi^I(0)\rangle$ . One can then obtain the time dependence of any observable O using the relation  $\langle O\rangle(t) = \langle \psi^I(t)|O^I(t)|\psi^I(t)\rangle$ . For our problem, we obtain  $V_{\rm eff} = H_{\rm XXZ,t} + H_{\rm XXZ,b} + \frac{1}{2}\sum_{\langle i,j\rangle}(\sigma_i^y\sigma_j^y + \sigma_i^z\sigma_j^z)$ . Remarkably, in this effective description, the three chains decouple into three separate integrable systems, and furthermore there now exists an emergent U(1) symmetry in the TFI chain which corresponds to arbitrary rotations around the x axis.

We are now equipped to calculate the local magnetization in the (bottom) XXZ chain and in the TFI chain. We anticipate a qualitative distinction between the XXZ and TFI magnetizations: The local magnetization operator in the XXZ chain  $\sigma_b^{z,I}(t) = U \sigma_b^z U^{\dagger} = \sigma_b^z$  is independent of time since Uand  $\sigma_h^z$  commute, while for the TFI chain it is explicitly time dependent,  $\sigma^{z,I}(t) = \sigma^z \cos(2ht) + \sigma^y \sin(2ht)$  (note that we suppressed the site labels to improve readability). Therefore the local magnetization in the XXZ chain  $\langle \sigma_h^z \rangle$  is fully determined by the quench dynamics in an integrable XXZ chain while in the TFI chain  $\langle \sigma^z \rangle$  will exhibit oscillations with period  $T = \pi/h$  in addition to its behavior determined by the TFI chain quench dynamics. As an example, we consider the case  $J_z = 0$ . Using results from Ref. [35], one finds  $\langle \sigma_b^z \rangle(t) \approx \cos(8J_x t - \pi/4)/\sqrt{t}$  for t < cL, where c is a constant. For t > cL, the finite-size effects take over and lead to oscillations whose time period is proportional to the finitesize gap  $\sim 8\pi J_x/L$ . Indeed, in our numerical simulations we observe systematic oscillations in the staggered magnetization  $m_z^{XXZ} \equiv \frac{1}{L} \sum_i (-1)^i \sigma_{i,t}^z$  of the XXZ subsystem with period  $T \approx \pi/(4J_x)$  [see Fig. 2(a)], which corresponds to L = 30. Since oscillations are cut off by finite-size effects at time O(L), we also studied much larger system size, L = 100, and found agreement with the prediction that  $T \approx \pi/(4J_x)$ —see the inset of Fig. 2(a). The same inset also shows the effect of including nonzero  $J_z = 0.5$ , in which case it is expected that the magnetization decays exponentially, modulated with weak oscillatory behavior [35], in line with our observation.

Turning next to the TFI chain, we find that the staggered magnetization  $m_z^{\text{TFI}} \equiv \frac{1}{L} \sum_i (-1)^i \sigma_i^z$  oscillates with period  $T = \pi/h$  in agreement with our prediction [Fig. 2(b)]. Two additional predictions of the prethermal physics encapsulated in  $V_{\text{eff}}$  can be made: (i) The emergence of the conserved quantities  $\chi^{yz} \equiv \frac{1}{L} \sum_{(i,j)} (\sigma_i^y \sigma_j^y + \sigma_i^z \sigma_j^z)$  and  $m_x^{\text{TFI}} \equiv \frac{1}{L} \sum_i \sigma_i^x$  and (ii) the decoupling of the three chains. We have verified numerically that the quantity  $\chi^{yz}$  remains constant after a quench to strong transverse field h = 15, as depicted in Fig. 2(c). Similarly, we also observe the conservation of  $m_x^{\text{TFI}}$  (see SM). To detect the decoupling of the three chains, we studied the entanglement between the top XXZ chain and the remainder of the system and find that it remains constant for sufficiently strong transverse field; see Fig. 2(d). By symmetry, the entanglement between the bottom chain and the remainder of the

system shows the same behavior, implying a decoupling of all three chains.

### VI. EXTENSIVE SUBSYSTEM DRIVE

We now consider a periodic steplike transverse field h(t)akin to the driving protocol illustrated in Fig. 1(c). During a single period T, we chose  $h(t) = h_{\text{max}}$  for t < T/2 and h(t) = 0 for T/2 < t < T. A translationally invariant closed quantum system subject to an external drive is generally expected to heat to infinite temperature in the long-time limit. A slow drive is indeed generally associated with fast heating. In contrast, the heating rate can become exponentially small in rapidly driven systems, resulting in long-lived prethermal states [31-34]. Such prethermalization behavior is typically studied when the whole system or a nonextensive subsystem is driven externally, and the case of an extensive subsystem drive has not received much attention. Here, we address the question of whether an extensive subsystem drive can also be associated with prethermal behavior and study how the system evolves under the slow ( $\omega = 0.5$ ) and fast ( $\omega = 5$ ) subsystem drives with  $h_{\text{max}} = 1.5$ . We first consider the case when the system is initially prepared in an eigenstate of the time-averaged Hamiltonian, i.e., it is an eigenstate of the equilibrium model with  $h(t) \equiv h_{\text{max}}/2$ . We keep track of three quantities during the time evolution: The magnetization, the bond dependence of the bipartition EE, and the QDL diagnostic for the effective entanglement between a single XXZ chain and the TFI chain.

For a slow drive ( $\omega=0.5$ ), the magnetization in both TFI and XXZ subsystems rapidly decays to half its initial value on the time scale of just a single period T. Over the course of approximately ten periods, the magnetization vanishes almost entirely, which is indicative of fast heating towards a trivial high-temperature paramagnetic state. In strong contrast, with the fast drive ( $\omega=5$ ) we find signatures of a long-lived prethermal state which preserves the finite magnetization of the ground-state configuration [Fig. 3(a)]. In both the TFI and XXZ subsystems a finite magnetization is maintained for more than 250 periods of the extensive subsystem drive, which is the maximum time duration in our numerical simulation.

We substantiate the qualitative difference between the slow drive and the fast drive by considering two different entanglement diagnostics. First, we calculate the dynamics of the bipartite EE, which reveals that under the slow drive the system becomes maximally entangled such that the EE scales as  $S_{\rm vN} = n \ln 2$  in the long-time limit, where n is the bond index in the matrix product state (MPS) representation of the system [Fig. 3(b)]. Such volume-law scaling of the EE is implied by a heating of the system to infinite temperature; note that the finite bond dimension  $\chi_{\text{max}}$  of the MPS causes a deviation from the scaling near the center (n = 15) of the chain when the EE approaches its theoretical upper bound ln  $\chi_{max}\approx 7.$  In the fast-driven case, when  $\omega = 5$ , the bipartite EE plateaus far before reaching the upper bound and does not seem to follow the volume law. This implies that the system does not thermalize within a moderate time scale, and the system instead remains in a prethermal phase. As a second entanglement measure we calculate the QDL diagnostic, which provides a more detailed characterization of entanglement in a multicomponent sys-

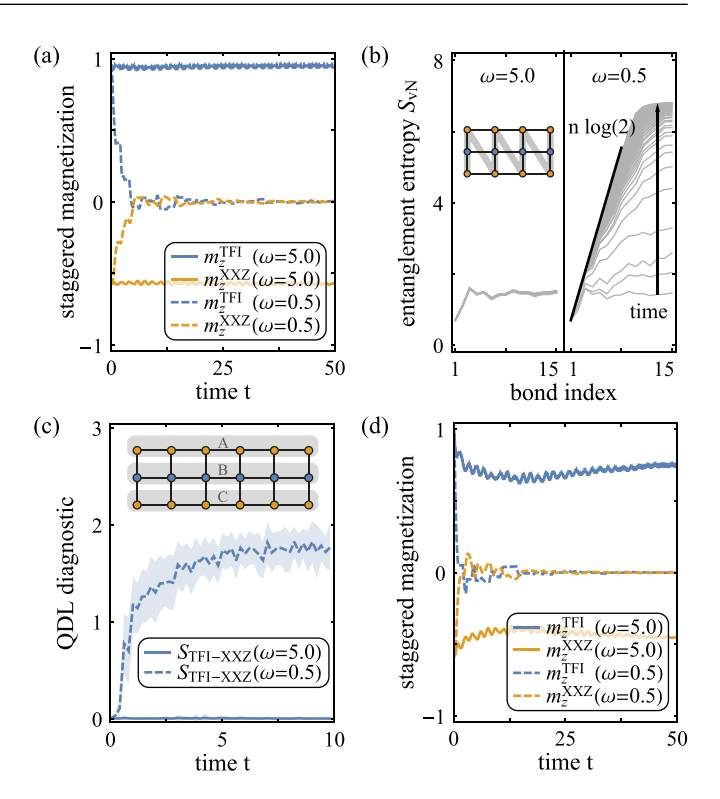


FIG. 3. Time evolution of the system under fast ( $\omega=5$ ) and slow ( $\omega=0.5$ ) periodic driving. Data shown are for L=30 and  $\chi_{max}=256$ . (a) Staggered magnetization in the XXZ and TFI subsystems. (b) Bipartition EE as a function of the bond index n, where n=1 denotes the end of the MPS and n=15 is the center; the inset shows the MPS structure used in this calculation. Data in this panel are for L=10 and  $\chi_{max}=1024$ . (c) QDL diagnostic for the effective entanglement between subsystems A and B shown in the inset. (d) Staggered magnetization in the XXZ and TFI subsystems when the initial configuration is not an eigenstate of the time-averaged Hamiltonian.

tem. Unlike the bipartite EE, the QDL diagnostic allows us to extract the effective entanglement between two *arbitrary* subsystems, which do not necessarily need to combine to the entire system. Let us consider  $S_{\text{TFI-XXZ}}$ , which corresponds to the entanglement between the top XXZ chain and the TFI chain after a projective measurement on the bottom XXZ chain [see the definition of the QDL diagnostic in Sec. III and the inset of Fig. 3(c)]. For the slow drive, we observe a steep growth in the QDL diagnostic, indicating that spins on each chain—which are close to a product state initially—become strongly entangled in a short time [Fig. 3(c)]. In contrast, for the fast drive, the QDL diagnostic remains vanishingly small for the entire time scale observed, in line with our expectations for a prethermal regime.

Finally, we briefly address the case when the initial configuration of the system is *not* an eigenstate of the time-averaged Hamiltonian. To this end, we prepare the system in the ground state of the equilibrium model at  $h(t) \equiv 0$  and subsequently apply the periodic drive. Generally, one would not expect a prethermal regime to arise. However, in analogy to the results discussed above, we still observe persistent magnetization for fast driving  $\omega = 5$ ; the steady-state magnetization is only slightly reduced when compared with its initial value [see

Fig. 3(d)]. We speculate that this rigidity against alteration of the initial configuration is a consequence of small variation of the ground-state wave function on finite-sized systems within the ordered phase of our three-chain model; for an isolated TFI chain, which shows greater variation throughout the ordered phase, such rigidity is not observed (see SM). We conclude that the environment of polarizable XXZ chains adds extra stability not only to the ground-state magnetization of the embedded TFI chain, but also to its time evolution.

#### VII. DISCUSSION

In this paper, we ask whether an interacting quantum system can enter a long-lived prethermal steady state when quantum-quench protocols or time-dependent drives are applied only to an extensive subsystem. Using the DMRG and TDVP for time evolution, we study the example of two XXZ spin chains coupled to a TFI chain, where only the TFI chain is quantum quenched or driven from a fully ordered ground state. In the case of sudden onset of the transverse field, when the strength of the transverse field is bigger than any other energy scale, it is shown that a prethermal steady state arises due to emergent quasiconservation laws. In a similar spirit, when a sufficiently fast time-dependent drive of the transverse field is applied, the system develops a prethermal state where the magnetization remains finite across the system and the entanglement between the spin chains remains small.

While the scenario of a prethermal state after a quantum quench is well captured within the framework of dynamic decoupling of chains [31,32], a universal description of the mechanism behind the formation of a prethermal state under a sufficiently fast extensive subsystem drive is currently lacking. However, we point out that the system under an extensive subsystem drive behaves like a fictitious substitute system that is subject to a global external drive: If the drive is slow, the system rapidly thermalizes, but if the drive is fast, the entanglement growth is impeded and the system enters a prethermal state. At least for a global external drive, such behavior is known to generalize across a large set of Hamiltonians. It remains an open question for future research whether our findings for an extended subsystem drive are similarly generalizable.

Our coupled spin-chain model is partly motivated by recent experiments on the organic material  $\kappa$ -H<sub>3</sub>(Cat-EDT-TTF)<sub>2</sub> ("H-Cat") and its deuterated analog. In those materials, layers of interacting electron systems (represented by XXZ spin chains in our model) are coupled via hydrogen bonds, where protons tunnel quantum mechanically in a double-well potential (spanned by bistable hydrogen bond configurations and modeled by transverse field Ising spins in our setup) with an intrinsic time scale. In first-principles calculations, the estimated tunnel barrier in H-Cat implies a tunneling rate of 10<sup>11</sup>–10<sup>14</sup> Hz [16]. While the actual tunneling rate may be affected by the presence of other molecules attached to the hydrogen bond [16], it is conceivable that the phonon-assisted optic mode associated with the hydrogen tunneling would couple to infrared light [36,37]. It would thus be interesting to explore whether an external optical drive in the infrared regime can be utilized to study the dynamic properties of H-Cat and the possibility to stabilize a prethermal regime (in the sense of our extensive subsystem drive model) in these organic compounds. Furthermore, if the tunneling rate of the hydrogen atoms can be tuned to be larger than all other scales, then even in the absence of any external driving, the system behaves as if it were being "self-driven" at a frequency given by the hydrogen tunneling rate. Therefore, if one prepares the system in the ground state of the symmetry-broken phase and evolves it with the time-independent Hamiltonian corresponding to a large tunneling rate, one still expects a prethermal symmetrybroken regime whose time now scales exponentially with the hydrogen tunneling rate.

#### ACKNOWLEDGMENTS

The numerical simulations were performed on the Cedar cluster, hosted by WestGrid and Compute Canada and implemented with the TeNPy library [38]. F.L.B. and Y.B.K. were supported by the NSERC and the Center for Quantum Materials at the University of Toronto. H.-Y.L. was supported by the National Research Foundation of Korea (Grant No. NRF-2020R1I1A3074769). T.G. acknowledges support from the National Science Foundation under Grant No. DMR-1752417 and from an Alfred P. Sloan Research Fellowship.

<sup>[1]</sup> J. Eisert, M. Friesdorf, and C. Gogolin, Quantum many-body systems out of equilibrium, Nat. Phys. 11, 124 (2015).

<sup>[2]</sup> T. Oka and S. Kitamura, Floquet engineering of quantum materials, Annu. Rev. Condens. Matter Phys. **10**, 387 (2019).

<sup>[3]</sup> M. S. Rudner and N. H. Lindner, The Floquet engineer's handbook, arXiv:2003.08252.

<sup>[4]</sup> A. Lazarides, A. Das, and R. Moessner, Equilibrium states of generic quantum systems subject to periodic driving, Phys. Rev. E 90, 012110 (2014).

<sup>[5]</sup> H. Kim, T. N. Ikeda, and D. A. Huse, Testing whether all eigenstates obey the eigenstate thermalization hypothesis, Phys. Rev. E 90, 052105 (2014).

<sup>[6]</sup> L. D'Alessio and M. Rigol, Long-Time Behavior of Isolated Periodically Driven Interacting Lattice Systems, Phys. Rev. X 4, 041048 (2014).

<sup>[7]</sup> A. Lazarides, A. Das, and R. Moessner, Periodic Thermodynamics of Isolated Quantum Systems, Phys. Rev. Lett. 112, 150401 (2014).

<sup>[8]</sup> V. Gritsev and A. Polkovnikov, Integrable Floquet dynamics, SciPost Phys. 2, 021 (2017).

<sup>[9]</sup> A. Lazarides, A. Das, and R. Moessner, Fate of Many-Body Localization Under Periodic Driving, Phys. Rev. Lett. 115, 030402 (2015).

<sup>[10]</sup> P. Ponte, Z. Papić, F. Huveneers, and D. A. Abanin, Many-Body Localization in Periodically Driven Systems, Phys. Rev. Lett. 114, 140401 (2015).

<sup>[11]</sup> J. Rehn, A. Lazarides, F. Pollmann, and R. Moessner, How periodic driving heats a disordered quantum spin chain, Phys. Rev. B 94, 020201(R) (2016).

- [12] J. Cayssol, B. Dóra, F. Simon, and R. Moessner, Floquet topological insulators, Phys. Status Solidi RRL 7, 101 (2013).
- [13] M. Bukov, L. D'Alessio, and A. Polkovnikov, Universal high-frequency behavior of periodically driven systems: from dynamical stabilization to Floquet engineering, Adv. Phys. 64, 139 (2015).
- [14] A. Eckardt, Colloquium: Atomic quantum gases in periodically driven optical lattices, Rev. Mod. Phys. 89, 011004 (2017).
- [15] F. Harper, R. Roy, M. S. Rudner, and S. Sondhi, Topology and broken symmetry in Floquet systems, Annu. Rev. Condens. Matter Phys. 11, 345 (2020).
- [16] K. Yamamoto, Y. Kanematsu, U. Nagashima, A. Ueda, H. Mori, and M. Tachikawa, Theoretical study of the H/D isotope effect on phase transition of hydrogen-bonded organic conductor κ-H<sub>3</sub>(Cat-EDT-TTF)<sub>2</sub>, Phys. Chem. Chem. Phys. 18, 29673 (2016).
- [17] M. Naka and S. Ishihara, Electronic state and optical response in a hydrogen-bonded molecular conductor, Phys. Rev. B **97**, 245110 (2018).
- [18] S. R. White, Density Matrix Formulation for Quantum Renormalization Groups, Phys. Rev. Lett. 69, 2863 (1992).
- [19] S. R. White, Density-matrix algorithms for quantum renormalization groups, Phys. Rev. B 48, 10345 (1993).
- [20] I. P. McCulloch, Infinite size density matrix renormalization group, revisited, arXiv:0804.2509.
- [21] J. Haegeman, J. I. Cirac, T. J. Osborne, I. Pižorn, H. Verschelde, and F. Verstraete, Time-Dependent Variational Principle for Quantum Lattices, Phys. Rev. Lett. 107, 070601 (2011).
- [22] T. Grover and M. P. A. Fisher, Quantum disentangled liquids, J. Stat. Mech.: Theory Exp. (2014) P10010.
- [23] J. R. Garrison, R. V. Mishmash, and M. P. A. Fisher, Partial breakdown of quantum thermalization in a Hubbard-like model, Phys. Rev. B **95**, 054204 (2017).
- [24] T. Veness, F. H. L. Essler, and M. P. A. Fisher, Quantum disentangled liquid in the half-filled Hubbard model, Phys. Rev. B 96, 195153 (2017).
- [25] D. Ben-Zion, J. McGreevy, and T. Grover, Disentangling quantum matter with measurements, Phys. Rev. B **101**, 115131 (2020).

- [26] See Supplemental Material at http://link.aps.org/supplemental/ 10.1103/PhysRevB.106.174417 for additional data and numerical details.
- [27] P. Pfeuty, The one-dimensional Ising model with a transverse field, Ann. Phys. (Amsterdam) **57**, 79 (1970).
- [28] H. C. Fogedby, The Ising chain in a skew magnetic field, J. Phys. C: Solid State Phys. 11, 2801 (1978).
- [29] F. C. Alcarez and A. L. Malvezzi, Critical and off-critical properties of the XXZ chain in external homogeneous and staggered magnetic fields, J. Phys. A: Math. Gen. 28, 1521 (1995).
- [30] Y. B. Kudasov and R. V. Kozabaranov, Variational model for one-dimensional quantum magnets, Phys. Lett. A 382, 1120 (2018).
- [31] D. Abanin, W. De Roeck, W. W. Ho, and F. Huveneers, A rigorous theory of many-body prethermalization for periodically driven and closed quantum systems, Commun. Math. Phys. 354, 809 (2017).
- [32] T. Mori, T. N. Ikeda, E. Kaminishi, and M. Ueda, Thermalization and prethermalization in isolated quantum systems: A theoretical overview, J. Phys. B: At., Mol. Opt. Phys. 51, 112001 (2018).
- [33] T. Mori, T. Kuwahara, and K. Saito, Rigorous Bound on Energy Absorption and Generic Relaxation in Periodically Driven Quantum Systems, Phys. Rev. Lett. 116, 120401 (2016).
- [34] D. A. Abanin, W. De Roeck, W. W. Ho, and F. Huveneers, Effective Hamiltonians, prethermalization, and slow energy absorption in periodically driven many-body systems, Phys. Rev. B 95, 014112 (2017).
- [35] P. Barmettler, M. Punk, V. Gritsev, E. Demler, and E. Altman, Quantum quenches in the anisotropic spin-Heisenberg chain: different approaches to many-body dynamics far from equilibrium, New J. Phys. 12, 055017 (2010).
- [36] A. J. Horsewill, Quantum tunnelling in the hydrogen bond, Prog. Nucl. Magn. Reson. Spectrosc. 52, 170 (2008).
- [37] T. Mochida, A. Izuoka, T. Sugawara, Y. Moritomo, and Y. Tokura, Organic hydrogen-bonded dielectrics: Quantum paraelectricity based on tautomerization of 9-hydroxyphenalenone derivatives, J. Chem. Phys. 101, 7971 (1994).
- [38] J. Hauschild and F. Pollmann, Efficient numerical simulations with Tensor Networks: Tensor Network Python (TeNPy), SciPost Phys. Lect. Notes **2018**, 5 (2018).